Study on Morphology and Viscoelastic Properties of PP/PET/SEBS Ternary Blend and their Fibers

N. Mostofi, H. Nazockdast, H. Mohammadigoushki

Polymer Engineering Department, Amirkabir University of Technology, Tehran, Iran

Received 10 August 2008; accepted 22 March 2009
DOI 10.1002/app.30612
Published online 17 August 2009 in Wiley InterScience (www.interscience.wiley.com).

ABSTRACT: The morphology development of polypropylene (PP)/polyethylene terephthalate (PET)/styrene-ethylene-butylene-styrene (SEBS) ternary blends and their fibers were studied by means of scanning electron microscopy (SEM) in conjunction with the melt linear viscoelastic measurements. The morphology of the blends was also predicted by using Harkin's spreading coefficient approach. The samples varying in composition with PP as the major phase and PET and SEBS as the minor phases were considered. Although SEM of the binary blends showed matrix-dispersed type morphology, the ternary blend samples exhibited a morphological feature in which the dispersed phase formed aggregates consisting of both PET and SEBS particles distributed in the PP matrix. The SEM of the blend samples containing 30 and 40 wt % of total dispersed phase showed an agglomerated structure formed between the aggregates. The SEM of the PP/PET binary fiber blends showed long well-oriented microfibrils of PET whereas in the ternary blends, the microfibrils were found to have lower aspect ratio with a fraction of the SEBS stuck on the microfibril fracture surfaces. These results were attributed to a core-shell type morphology in which the PET and SEBS formed the core-shells distributed in the matrix. The melt viscoelastic behavior of the ternary blends containing less than 30 wt % of the total dispersed phase was found to be similar to the matrix and binary blend samples whereas the samples containing 30 and 40 wt % of dispersed phases exhibited a pronounced viscosity upturn and nonterminal storage modulus in low frequency range. These results were found to be in good agreement with the morphological results. J Appl Polym Sci 114: 3737–3743, 2009

Key words: ternary blends; core-shell morphology; microfibrillar morphology; viscoelastic properties

INTRODUCTION

The blending of two or more different polymer has widely been used as a flexible and economical technique for production of polymeric materials with desirable properties. During the last two decades, a considerable number of researches have been conducted toward multicomponent polymer blends consisting of at least three or more immiscible polymers. A large range of phase morphologies can be generated, which could directly influence the whole set of properties.[1–5] The effect of different parameters on the morphology and properties of ternary polymer blends have been studied by many researchers. Hobbs et al.[1] used Harkin's spreading coefficient concept[6] to predict the phase morphology of different ternary blends. For a ternary system with *A* as the continues phase and *B* and *C* as the dispersed phases, the spreading coefficients λ_{BC} and λ_{CB} are defined as:

$$\lambda_{BC} = \gamma_{AC} - \gamma_{AB} - \gamma_{BC} \quad (1)$$

$$\lambda_{CB} = \gamma_{AB} - \gamma_{AC} - \gamma_{BC} \quad (2)$$

where γ_{ij} is the interfacial tension between *i* and *j* phases. A positive value of λ_{BC} and negative value of λ_{CB} will lead to encapsulation of *C* phase by the *B* phase. If λ_{BC} and λ_{CB} are both negative, two minor components form separate dispersed phases. In the case, both λ_{CB} and λ_{BC} are negative and λ_{AC} is positive one phase will partially encapsulate the other phase.[7]Guo et al.[8] also developed a model to predict phase morphologies of multiphase polymer blends based on minimizing the relative interfacial free energy (RIE). According to these, Model 3 morphologies namely as: (1) two minor Phases *B* and *C* disperse separately (*B* + *C*). (2) Phase *B* encapsulates Phase *C* (*B/C*). (3) Phase *C* encapsulates Phase *B* (*C/B*) are available. The interfacial free energy of each of these morphologies are expressed as follows:

$$G = \sum_i n_i \mu_i + \sum_{i \neq j} A_i \gamma_{ij} \quad (3)$$

$$G_{B+C} = (n_1\mu_1 + n_2\mu_2 + n_3\mu_3) + (A_{B_{B+C}}\gamma_{AB} + A_{C_{B+C}}\gamma_{AC}) \quad (4)$$

$$G_{B/C} = (n_1\mu_1 + n_2\mu_2 + n_3\mu_3) + (A_{B_{B/C}}\gamma_{AB} + A_{C_{B/C}}\gamma_{BC}) \quad (5)$$

Correspondence to: H. Nazockdast (nazdast@aut.ac.ir).

$$G_{C/B} = (n_1\mu_1 + n_2\mu_2 + n_3\mu_3) + (A_{B_{C/B}}\gamma_{BC} + A_{C_{C/B}}\gamma_{AC}) \quad (6)$$

$$\left(\sum A_i\gamma_{ij}\right)_{B+C} = (4\pi)^{1/3}[n_B^{1/3}x^{2/3}\gamma_{AB} + n_C^{1/3}\gamma_{AC}](3V_C)^{2/3} \quad (7)$$

$$\left(\sum A_i\gamma_{ij}\right)_{B/C} = (4\pi)^{1/3}\left[n_B^{1/3}(1+x)^{2/3}\gamma_{AB} + n_C^{1/3}\gamma_{AC}\right](3V_C)^{2/3} \quad (8)$$

$$\left(\sum A_i\gamma_{ij}\right)_{C/B} = (4\pi)^{1/3}\left[n_B^{1/3}x^{2/3}\gamma_{BC} + n_C^{1/3}(1+x)^{2/3}\gamma_{AC}\right](3V_C)^{2/3} \quad (9)$$

$$x = \frac{V_B}{V_C} \quad (10)$$

where the G is the free energy of the blends, V_B and V_C are the volume of the dispersed Phases B and C, respectively. n_B and n_C are the number of particles of dispersed Phases B and C. Because the term $\sum_i n_i u_i$ in eqs. (3)–(6) are related to bulk properties and have constant values, they can be omitted. On the basis of this model, the dominating morphology will be that with minimum relative interfacial energy.

Reignier et al.[9] developed a conceptual model to predict encapsulation effects in composite type systems based on the same model but using dynamic interfacial tension proposed by Van Oene.[10]

The formation of subinclusions in a ternary blend was related to the inability of particles to disperse in the matrix due to the high viscosity of dispersed phase.[11] Kim et al.[12] showed that in ternary blends with core-shell morphology the minor phase with lower viscosity tends to encapsulate the other minor phase. Luzinov et al.[13] demonstrated that in PS/SBR/polyethylene terephthalate (PET) blends, the size of PET core is proportional to the viscosity ratio of the PET core to SBR shell. In another study, Hemmati et al.[14] showed that in polypropylene (PP)/PE/EPDM ternary systems the composite droplet size is proportional to the ratio of average viscosity of complex droplet to that of matrix. Reignier and Favis[15] reported that for the HDPE/PS/PMMA ternary blends there is a critical shell volume fraction, above which the PS/PMMA composite droplet exhibits pure PS droplet behavior. Hemmati et al.[16] also showed that in ternary blends with core-shell morphology the size of core as well as composite droplets increases with increasing the core content while in the systems, in which both phases are dispersed separately, the size of each dispersed phase is not only determined by concentration but also by viscosity and the interfacial tension of that phase with matrix.

Processing of an incompatible polymer pair, in which the dispersed phase forms *in situ* microfibrils, called as microfibril reinforced composites (MFC), has been known as a new way to achieve products with very high mechanical properties.[17–20] One of the best ways to achieve this goal is to blend thermoplastics with thermo tropic liquid crystalline polymers (TLCP). Many researches have been focused on parameters affecting the microfibrillar morphology development and mechanical properties of MFCs.[21,22,17] Friedrich et al.[17] investigated the morphology and mechanical properties of microfibrillar reinforced composites based on PP/PET blends. Similar work was carried out on PP/PA MFC by Afshari et al.[23] Fuchs et al.[24] found a good agreement between the tensile properties of these materials and the values predicted by Tsai-Hill equation.

The aim of the present work is to study the relationship between morphology and the melt linear viscoelastic properties of PP/PET/styrene-ethylene-butylene-styrene (SEBS) ternary blends and the fibers produced from the blends.

EXPERIMENTAL

Materials

A commercial fiber grade PP, (V30S) with MFI = 18 g/10 min (230°C/2.16 kg), supplied by Arak Petrochemical Co. in Iran, was used as major component. A fiber grade PET supplied by Yazd polyester Co. and a SEBS copolymer (Kraton G1652) and a SEBS copolymer grafted with 2% of maleic anhydride (Kraton FG1901X) both supplied by Shell Chemicals were used as second minor phase. In both triblock, copolymers used the ratio of Styrene to ethylene/Butylene was 30/70 by weight.

Blend preparation

The PET resins were dried in an oven at temperature of 100°C for 24 h before melt blending to minimize the hydrolytic degradation of polyester. All the blend samples were prepared in a 60CC Brabender internal mixer equipped with roller type rotors at 275°C and 75 rpm.

Fiber preparation

The ternary blend samples were melt spun by using a Brabender single screw extruder with screw equipped with a 20 holes spinneret. The temperature zones of the barrel from the hopper to the spinneret were set at 170, 190, 210, 220, 230°C.

Morphological study

Morphology of the blends sample and blend fibers were studied using a Philips scanning electron microscopy (SEM). The SEM micrographs were taken from cryogenically fractured surfaces of the blend samples and fiber sections. All the fractured surfaces were coated with a thin layer of gold before viewing.

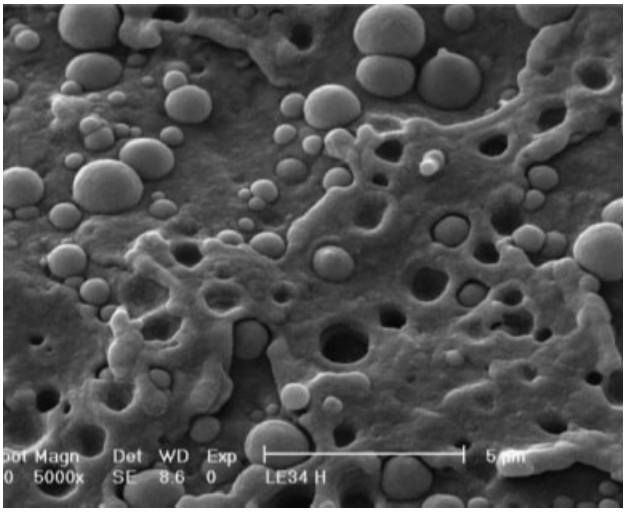

Figure 1 SEM micrograph of 86/14 (wt/wt) binary blend of PP/PET.

Rheological measurements

The linear melt viscoelastic properties of the blend components and the blend samples were carried out using a rheometric mechanical spectrometer (RMS) equipped with a parallel plate with a gap of 1 mm and a plate diameter of 25 mm. The measurements were performed at constant amplitude of 1%, in the frequency range of 0.1–6251/s at 275°C under dry nitrogen atmosphere.

RESULTS AND DISCUSSION

Morphology

Figure 1 shows a typical SEM micrograph of PP/PET binary blend samples. The relatively large particle size with coarse particle size distribution of PET dispersed in PP matrix can be considered as indications of incompatibility and therefore weak interfacial interaction between these two phases.

Figure 2 shows the SEM micrographs of PP/PET/SEBS and PP/PET/SEBS-g-MA ternary blend samples with composition of 80/14/6. As it can be clearly seen, the both samples show a morphological feature in which the minor phases form well defined aggregates dispersed in the PP matrix. Figure 3 presents the morphology of the PP/PET/SEBS and PP/PET/SEBS-g-MA ternary blend samples with the same composition of 60/28/12. As can be noticed in

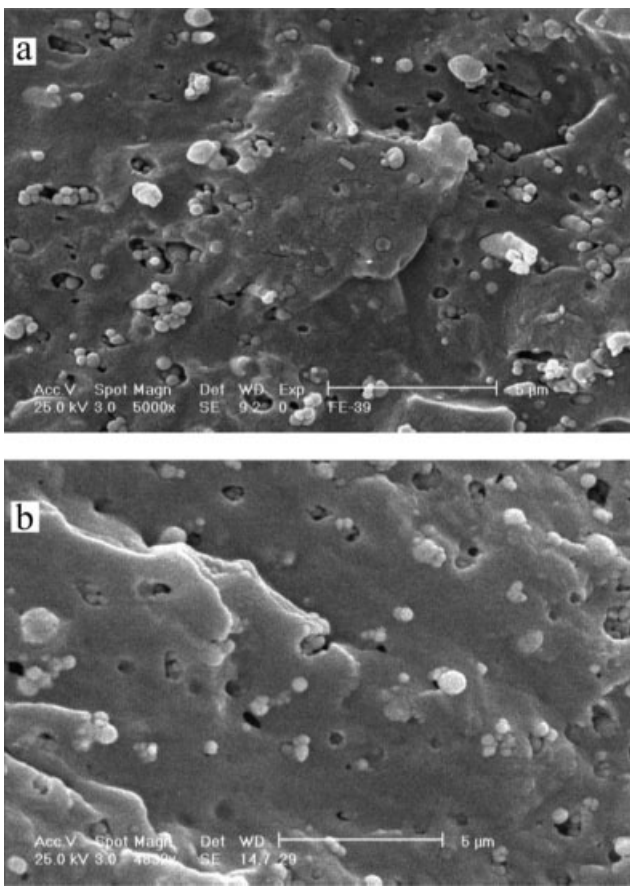

Figure 2 SEM micrograph of ternary blends containing (a) PET (14% wt) and SEBS (6% wt), (b) PET (14% wt) and SEBS-g-MA (6% wt).

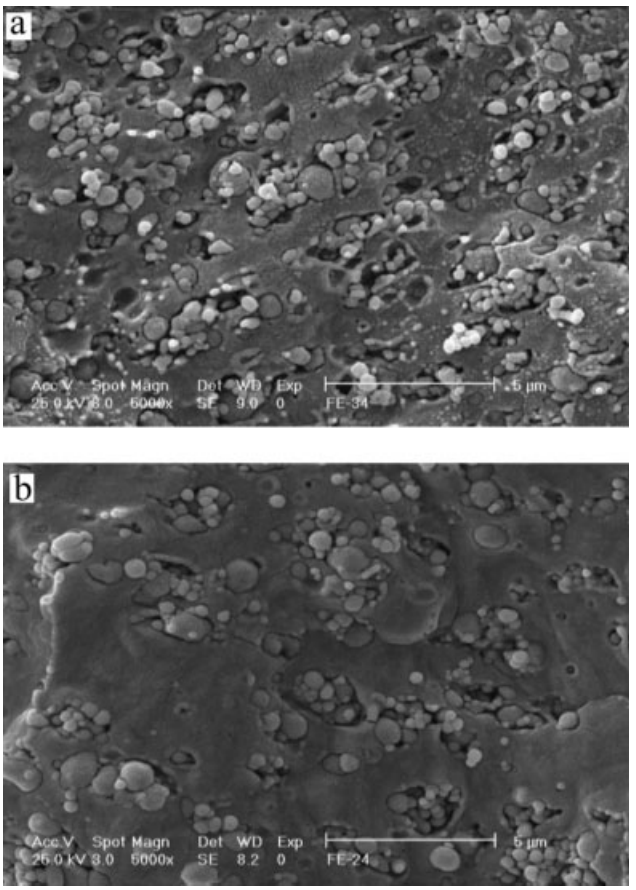

Figure 3 SEM micrographs of ternary blends containing (a) PET (28% wt) and SEBS (12% wt), (b) PET (28% wt) and SEBS-g-MA (12% wt).

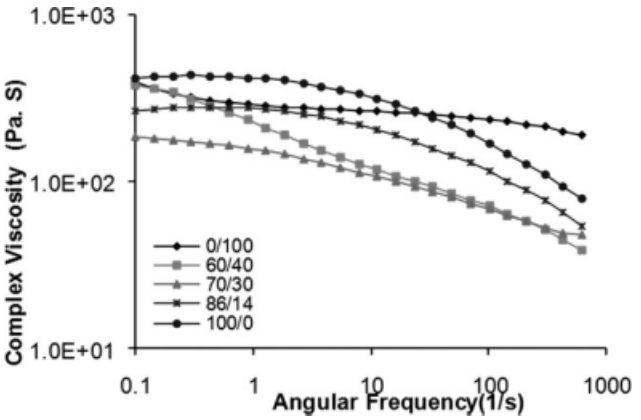

Figure 4 Complex viscosity vs. angular frequency for PP/PET binary blends at $T = 275°C$. Blend compositions are described in figure.

both samples, the aggregates formed between particles are interconnected into 3D agglomerates. Comparing these results showed that SEBS and SEBS-g-MA play an almost similar role in morphology development in these samples.

Because the two minor phases PET and SEBS are immiscible and both are immiscible with the PP matrix, the aggregate formed between the dispersed phases can be attributed to formation of a core-shell type morphology in which the PET is encapsulated by highly elastic SEBS phase. The morphology with aggregate formation was also observed for PP/PA6/SEBS ternary blend system by Wilkinson[25] who also attributed the aggregate formation to core/shell-type morphology.

Rheology

The results of complex viscosity (η*) vs. angular frequency of PP, PET, and their binary blends are shown in Figure 4. Although the samples containing less than 40% wt of PET showed a flow behavior similar to that of PP matrix, the flow behavior of the binary blend sample with 40% wt of PET at low frequency range could not be superimposed with that of PP and showed a low frequency non-Newtonian response. This could be related to the co-continues type morphology developed in this particular sample.

The results of storage modulus (G') vs. angular frequency obtained for the ternary blend samples containing 20% of total minor phase and binary blend containing the same amount of minor phase is shown in Figure 5. As it can be seen, the ternary blend sample shows a pronounced nonterminal storage modulus at low frequency range. Moreover, the values of low frequency storage modulus of ternary blend samples were found to be greater than those predicted by Palierne[26] model, proposed for binary blends and by considering the core-shell droplet as a single droplet with weighted average viscoelastic properties of the minor components. The interfacial interaction of our sample was calculated on the basis of interfacial interaction between PP matrix and SEBS shell. As it can be seen in Figure 6, the ternary blend sample exhibit a distinct positive deviation from Palierne model. Moreover, the frequency range, below which the elastic response of our ternary blend samples begins, is much higher than those reported for binary blends.[27,28] Therefore, the enhanced low frequency elastic response of this ternary blend sample can be attributed to core-shell morphology and resulting aggregates formed in this sample.

Figure 7 presents the storage modulus (G') and complex viscosity (η*) as a function of frequency for the two ternary blend samples containing 30% and 40% wt/wt of total minor phase. As can be clearly

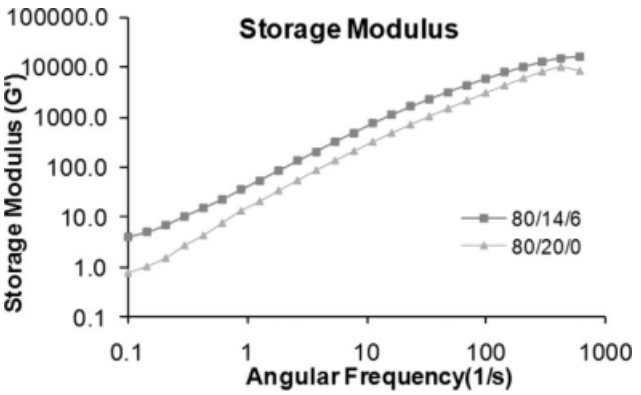

Figure 5 Rheological behavior of PP/PET/SEBS ternary blends and PP/PET binary blend at $T = 275°C$: Storage modulus vs. angular frequency.

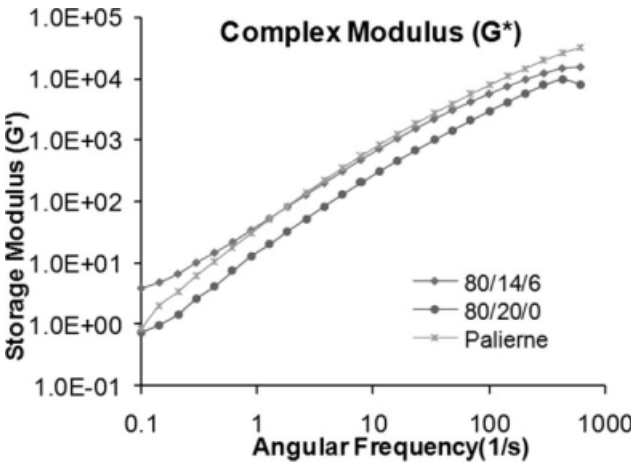

Figure 6 Rheological behavior of PP/PET/SEBS ternary blends and PP/PET binary blend at $T = 275°C$: Complex modulus vs. angular frequency compared to the Palierne model.

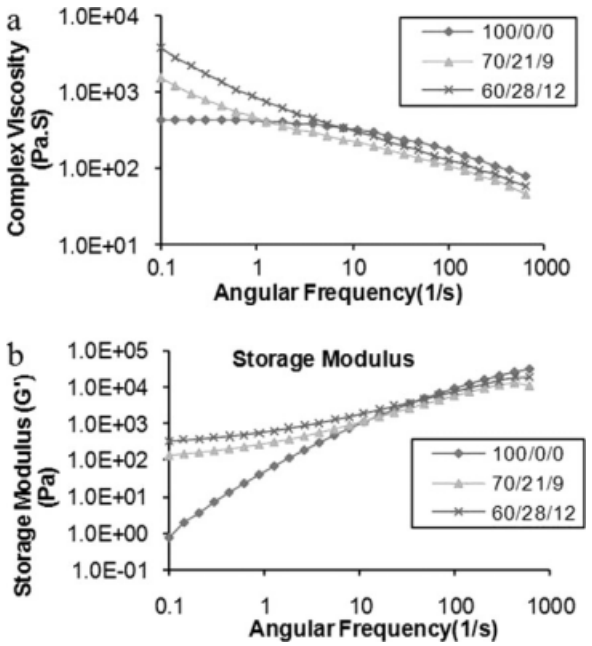

Figure 7 Rheological behavior of PP/PET/SEBS ternary blends at $T = 275°C$: (a) complex viscosity (η^*) and (b) storage modulus (G') vs. angular frequency. The blend compositions are described in figure.

seen, these samples exhibit a pronounced viscosity upturn and strong nonterminal storage modulus at low frequency range. The values of low frequency storage modulus were found to be in the range of those reported for concentrated suspensions[29] with 3D agglomerate structure. In other words, these results were in good agreement with aggregates or agglomerate structure development resulting from core-shell type morphology in these ternary blend samples. A similar behavior was reported for a 50/50 matrix/core-shell type modifier polymer blend consisting of PBA as core that is grafted with PMMA shell dispersed in PMMA matrix by Choi et al.[28] who attributed their results to strong interfacial adhesion as a result of trapping the matrix chains in the shell and resulting interconnectivity of the dispersed particles. However, this explanation could not be applied to our sample that had agglomerate microstructure.

Figure 8(a) shows the results of melt viscoelastic properties of PP/PET/SEBS-g-MA sample performed at 180°C at which the PET phase remain in its solid state. The superposition of these results with those obtained at 275°C [Fig. 8(b)] can be considered as an indication that in both cases PET phase does not play an appreciable role in determining the viscoelastic properties of these samples. Therefore, these results can be considered as evidences to support the above suggested core-shell type morphology in which the SEBS with high melt elasticity encapsulates the PET phase.

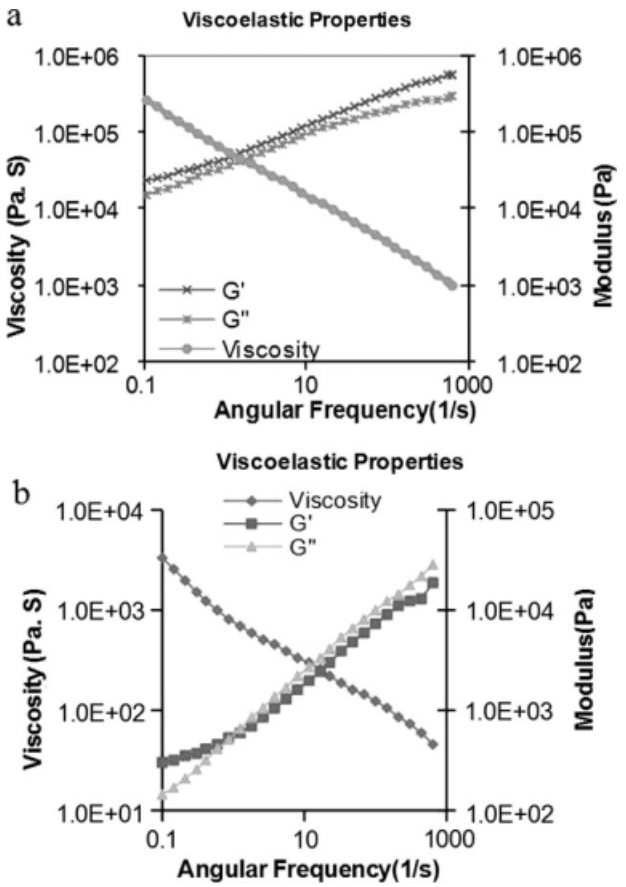

Figure 8 Viscoelastic properties of ternary blend with concentration PP/PET/SEBS-g-MA = 60/28/12 at (a) $T = 180°C$, (b) $T = 275°C$.

Figure 9 shows SEM micrograph of a PP/PET binary blend filament with concentration of 86/14 which was etched by boiling xylene. As it can be seen, the PET phase is drawn into long fibrils with a high *L/D* ratio in the fibers. A similar morphology has been observed by other researches elsewhere.[30]

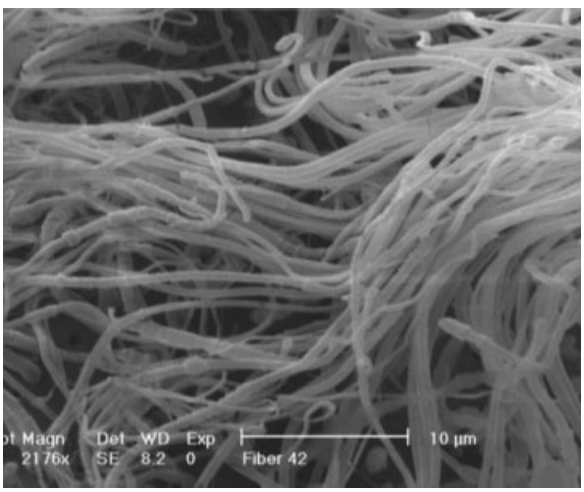

Figure 9 SEM micrograph of binary PP/PET fiber.

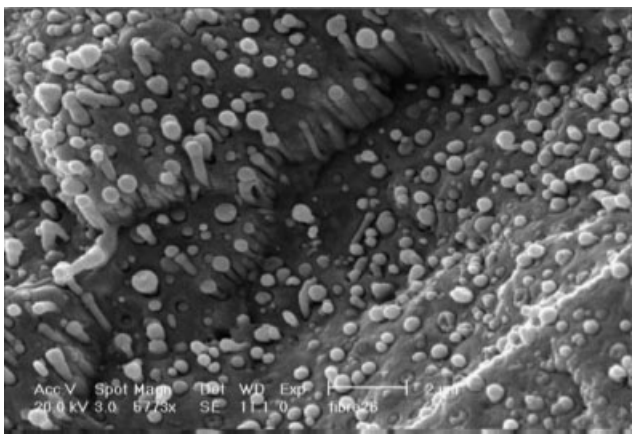

Figure 10 The SEM micrograph of PP/PET/SEBS ternary blend with concentration of 60/28/12 fiber blend.

The SEM micrograph of cryogenically fractured surface of PP/PEP/SEBS ternary blend fibers is shown in Figure 10. Comparing these results with those shown in Figure 9, one can notice that while in PP/PET binary blend fibers the PET droplets form long microfibrils, in PP/PET/SEBS ternary fibers the minor phase is drawn into short fibrils with lower aspect ratio whose broken surface are covered by SEBS phase which may probably be formed after breaking of fibrils during cryogenic fracturing of the filament samples. These results support our above discussed suggestion, stating that SEBS phase encapsulates the PET because there is no sign of SEBS dispersed phase and only one kind of microfibrils can be observed. The lower aspect ratio of the fibrils observed in compatibilized samples can be explained in terms of reduced droplet size and therefore less deformability of droplets in these samples. Thus, SEBS phase acts as highly elastic resisting skin for the core shell to be drawn into long fibrils. Thus, it can be suggested that the core/shell droplets formed in the blend samples is drawing into core/shell type fibrils in the spun fibers during the melt spinning.

The morphology of these blends was also predicted by using the spreading coefficient concept and relative interfacial energy (RIE). First, interfacial tensions (γ_{ij}) data were calculated for the three polymer–polymer interfaces present in the blends, i.e., PP-PET, PP-SEBS, and PET-SEBS using the harmonic mean equation.[31]

$$\gamma_{ij} = \gamma_i + \gamma_j - \frac{4\gamma_i^d \gamma_j^d}{\gamma_i^d + \gamma_j^d} - \frac{4\gamma_i^p \gamma_j^p}{\gamma_i^p + \gamma_j^p} \tag{11}$$

where γ_{ij} is the interfacial tension between Components i and j, γ_i is the surface tension of Component i, γ_i^{d} and γ_i^{P} are dispersive fraction and polar fraction of surface tension of the component i, respectively. The data used in these calculations are shown in Table I. For the purpose of this calculation, the SEBS triblock copolymer was considered as a random ethylene-butylene(r-EB) copolymer, because the SEBS structure is dominated by the central EB-block (block molecular weights: 7000S-37500EB-7000S).[31]

The values of interfacial tension of the blend components at 275°C calculated using eq. (11) were $\gamma_{\mathrm{PP/PET}} = 6.58$, $\gamma_{\mathrm{PET/SEBS}} = 4.99$, $\gamma_{\mathrm{SEBS/PP}} = 1.26$.

The calculated values of interfacial tensions were used to obtain the spreading coefficient and relative interfacial energy (RIE) values using eqs. (1) and 2 and also eq. (3) to predict the morphology of the PP/PET/SEBS ternary polymer blends. The spreading coefficient values calculated for blends containing SEBS are: $\lambda_{\mathrm{SEBS/PET}} = 0.33$, $\lambda_{\mathrm{PET/SEBS}} = -10.31$. From these values, one may think that the driving force of SEBS is too small to encapsulate PET. However, in the above described model the static interfacial tension was considered. Although as Van Oene[10] suggested that interfacial tension under the conditions of dynamic flow can be quiet different from that of the static one due to difference in blend components elasticity. Reignier et al.[9] introduced the dynamic interfacial term for polymer blends based on the Van Oene equation to predict the morphology of ternary blend. According to Reignier, when the melt elasticity of the blend matrix is greater than that of dispersed phase γ_{12} will fall with increasing shear and will rise when the melt elasticity of the blend matrix is less than that of dispersed phase. Results of melt viscoelastic properties obtained for polymer components as discussed earlier showed that the melt elasticities of the blend components are in the order of SEBS $\approx$ SEBS-g-MA>PP>PET. Therefore, these results that are in agreement with

TABLE I
Data for Calculating Values of Interfacial Tension for Ternary Blends

Polymer	γ (mN m^{-1})	γ^{d} (mN m^{-1})	γ^{P} (mN m^{-1})	$d\gamma/dT$ (mN m^{-1}°C)	Reference
PP	15.3	14.99	0.31	−0.065	30
PET	28.0	21.81	6.19	−0.058	30
r-EB	22.2	21.76	0.44	−0.045	31

experimental results suggest that PET phase is encapsulated by SEBS phase.

The calculated values of RIE for the samples in 275°C are as follows:

$$\mathrm{RIE(PET/SEBS)} = 18.2$$

$$\mathrm{RIE(PET + SEBS)} = 7.7$$

$$\mathrm{RIE(SEBS/PET)} = 7.6$$

As it can be also seen, the morphology which SEBS encapsulates the PET has the lowest free energy indicating that the SEBS phase will encapsulate the PET phase.

CONCLUSIONS

Although SEM micrographs of the PP/PET binary blends showed matrix-dispersed type morphology, the ternary PP/PET/SEBS blend samples exhibited a different morphological feature in which the dispersed phase formed distinct aggregates consisting of both PET and SEBS particles distributed in the PP matrix. The SEM micrographs of the blend samples containing 30 and 40 wt % of total dispersed phase showed an agglomerated structure formed between the aggregates. These results could be attributed to the core-shell type morphology in which PET was encapsulated by SEBS phase. The SEM micrographs of the PP/PET binary blend fibers showed long microfibrils of PET well oriented along the fiber axes whereas in the case of ternary blends, the microfibrils were found to be shorted with larger diameter with a fraction of the SEBS phase stuck on the microfibril fracture surfaces resulting from SEBS shell rupture. These results also revealed the core-shell morphology type for the ternary polymer blends.

The melt-state viscoelastic behavior of the ternary blends containing less than 30 wt % of the total dispersed phase was found to be similar to PP matrix and binary blend samples, whereas the samples containing 30 and 40 wt % of total dispersed phase exhibited a pronounced viscosity upturn and storage nonterminal behavior in low frequency region. These results, which are in good agreement with the SEM results, suggest a core-shell type morphology for molten PP/PET/SEBS ternary blend in which the SEBS with high melt elasticity encapsulates the PET phase. A good agreement was found between the experimental results and the results predicted by Harkin's spreading equation.

References

1. Hobbs, S. Y.; Dekkers, M. E. J.; Watkins, V. H. Polymer 1988, 29, 1598.
2. Nemirovsky, N.; Siegmann, A.; Narkis, N. J Macromol Sci Phys 1995, 34, 459.
3. Horiuchi, S.; Matchariyakul, N.; Yase, K.; Kitano, T.; Choi, H. K.; Lee, Y. M. Polymer 1996, 37, 3065.
4. Horiuchi, S.; Matchariyakul, N.; Yase, K.; Kitano, T.; Choi, H. K.; Lee, Y. M. Polymer 1997, 38, 59.
5. Rosch, J. Polym Eng Sci 1995, 35, 1917.
6. Harkin, W. D. The Physical Chemistry of Surface Films; Reinhold: New York, 1952.
7. Joel Reignier, B. D. Macromolecules 2000, 33, 6998.
8. Guo, H. F.; Packirissamy, S.; Gvozdic, N. V.; Meier, D. J. Polymer 1997, 38, 785.
9. Reignier, J.; Favis, B. D.; Heuzey, M. C. Polymer 2003, 44, 49.
10. Van Oene, H. J Colloid Interf Sci 1972, 40, 448.
11. Favis, B. D.; Chalifoux, J. P. Polymer 1988, 29, 1761.
12. Kim, B. K.; Kim, M. S.; Kim, K. J. J Appl Polym Sci 1993, 48, 1271.
13. Luzinov, I.; Pagnoulle, C.; Xi, K.; Huynh-Ba, G.; Jerome, R. Polymer 1999, 40, 2511.
14. Hemmati, M.; Nazokdast, H.; Shariatpanahi, H. J Appl Polym Sci 2001, 82, 1129.
15. Reignier, J.; Favis, B. D. Polymer 2003, 44, 5061.
16. Hemmati, M.; Nazokdast, H.; Shariatpanahi, H. J Appl Polym Sci 2001, 82, 1138.
17. Friedrich, K.; Evstatiev, M.; Fakirov, S.; Evstatiev, O.; Ishii, M.; Harrass, M. Comp Sci Tech 2005, 65, 107.
18. Evstatiev, M.; Fakirov, S. Polymer 1992, 33, 877.
19. Fakirov, S.; Evstatiev, M. Macromolecules 1993, 26, 5219.
20. Fakirov, S.; Evstatiev, M. Adv Mater 1994, 6, 395.
21. Dencheva, N.; Nunes, T.; Jovita Oliveira, M.; Denchev, Z. Polymer 2005, 46, 887.
22. Sarkissova, M.; Harrats, C.; Groeninchkx, G.; Thomas, S. Compos Part A: Appl Sci Man 2004, 35, 489.
23. Afshari, M.; Kotek, R.; Haghighat Kish, M.; Nazockdast, H.; Gupta, B. S. Polymer 2002, 43, 1331.
24. Fuchs, C.; Bhattacharyya, D.; Fakirov, S. Compos Sic Tech 2006, 66, 3161.
25. Wilkinson, A. N.; Clemens, M. L.; Harding, V. M. Polymer 2004, 45, 5239.
26. Palierne, J. F. Rheol Acta 1990, 29, 204.
27. Bousmina, M.; Muller, R. J Rheol 1993, 37, 663.
28. Choi,J.-H.; Ryu, J.-H.; Kim, S.Y. J Polym Sci Part B: Polym Phys 38, 942.
29. Shenoy, V. Rheology of Filled Polymer Systems; Kluwer Academic Publishers: Dordrecht, The Netherlands, 1999.
30. Afshari, M.; Kotek, R.; Gupta, R. S.; Haghighatkish, M.; Nazock Dast, H. J Appl Polym Sci 2005, 97, 532.
31. Wu, S. Polymer Interface and Adhesion Marcel Decker: New York, 1982.